Solar-Terrestrial Physics. 2023. Vol. 9. Iss. 2. P. 55–65. DOI: 10.12737/stp-92202307. © 2023 V.L. Yanchukovsky. Published by INFRA-M Academic Publishing House

UDC 524.1
DOI: 10.12737/stp-92202307

Received February 16, 2023
Accepted March 23, 2023

TEMPERATURE EFFECT OF MUONS REGISTERED UNDER THE GROUND IN YAKUTSK BY TELESCOPES ON GAS-DISCHARGE COUNTERS

V.L. Yanchukovsky
A.A. Trofimuk Institute of Oil and Gas Geology and Geophysics SB RAS,
Novosibirsk, Russia, YanchukovskiyVL@ipgg.sbras.ru

Abstract. The Yakutsk spectrograph of cosmic rays includes a complex of muon telescopes based on gas-discharge and scintillation counters located on the surface and under the ground at depths of 7, 20, and 40 m.w.e. Using continuous observations made by muon telescopes on gas-discharge counters and data on the altitude profile of the atmospheric temperature over Yakutsk for the period from January 2016 to December 2018, we have calculated density distributions of temperature coefficients for muons detected on the surface and at various depths under the ground. To do this, we employed multivariate regression methods and principal component methods. The results obtained are compared with the results of earlier theoretical calculations. The results make it possible to correctly take into account the temperature effect in the data from the complex of muon telescopes on gas-discharge counters.

Keywords: cosmic rays, atmosphere, muons, telescope, temperature effect.

INTRODUCTION

Variations in the intensity of cosmic rays (CRs) of atmospheric origin are caused by variations in atmospheric parameters (pressure, temperature, humidity, mass redistribution) [Dorman, 1972]. The contribution of these parameters to the atmospheric CR variation for different components of secondary CRs differs. For the meson component, which consists of unstable particles, the temperature effect is decisive, although there is also a weak barometric effect. For effective use of muon telescope data, we should adequately take into account the contribution of atmospheric variations [Yanchukovsky, Kuzmenko, 2018]; to do this, it is first necessary to estimate the effect of various atmospheric parameters on the intensity of muons. The barometric effect of the muon intensity is determined by the pressure at the observation level and therefore is found and taken into account quite simply. The temperature variation in the muon intensity depends on many parameters that characterize the air temperature regime from the layer of generation of muons to the level of their detection.

The integral method of accounting for the temperature effect [Dorman, 1957] is almost free from weaknesses since it involves considering the entire air temperature profile and takes into account the mass distribution, which is completely and unambiguously controlled by the temperature profile of the atmosphere from the observation level to its boundary. The integral method requires regular data on aerological sounding and temperature coefficient density distribution for atmospheric muons. Temperature coefficient densities for muons have been obtained earlier from theoretical calculations by many authors [Dorman, Janke, 1971; Berkova et al., 2008; Dmitrieva et al., 2009; Kuzmenko, Yanchukovsky, 2017]. In particular, calculations were made for Novosibirsk muon telescope/hodoscope and Yakutsk underground complex of muon telescopes [Kuzmenko, Yanchukovsky, 2017]. The results of theoretical calculations should be carefully used to correct observational data because they are made with certain approximations. Effective use of the integral method [Dorman, 1972] suggests knowing how the temperature coefficient density is distributed in a specific experimental facility.

It is also difficult to estimate the temperature coefficient density from observational data because temperature variations in different atmospheric layers are correlated. We have therefore used different data analysis methods for the complex of underground muon detectors in Yakutsk to determine the temperature coefficients from continuous observations.

DATA

The cosmic ray spectrograph after A.I. Kuzmin in Yakutsk [Starodubtsev et al., 2016; Gerasimova et al., 2021] includes a 24NM-64 neutron monitor and a complex of muon detectors located on Earth's surface and under the ground at levels of 7, 20, and 40 m w.e. and providing muon detection from the vertical, N30, S30, N60, and S60 directions. The altitude of the CR station Yakutsk (61.59° N, 129.41° E) is 95 m; the geomagnetic cutoff rigidity is 1.65 GV.

We have used raw hourly continuous observations from the complex of muon detectors on gas-discharge counters, the neutron monitor [https://ikfia.ysn.ru/data/hecrlab/mt; https://ikfia.ysn.ru/data/h ecrlab/ipm], as well as atmospheric pressure data for the period from January 2016 to December 2018. Vertical atmospheric temperature profiles (for each hour) over Yakutsk were taken from the database [http://crsa.izmiran.ru/phpmyadmin], which contains the results of the US National Center for Environmental Prediction (NCEP) [https://www.nco.ncep.noaa.gov/pmb/products/gfs].

In order to visually control the raw data, we have plotted all detection channels and ratios of identical channels (30N/30S, 60N/60S). No discrepancies were found and hence no trend assessment was carried out. The outliers we found were removed, and the existing gaps in the raw hourly data (September 29 and 30, 2016, as well as October 30, 2018) were filled with the averages calculated from four values both before and after each gap. Using the Yakutsk neutron monitor data for the period from January 2016 to December 2018, we estimated the barometric coefficient by the pair correlation method: –0.73±0.004 %/mb, whereas according to [https://ikfia.ysn.ru/data/hecrlab/ipm] the barometric coefficient is 0.723 %/mb. Hereinafter, a new value of the barometric coefficient will be used for the neutron monitor in Yakutsk.

All the raw data were reduced to daily averages whose total number was:

- 1077 for the ground telescope (MT00);
- 1033 for the telescope at the level of 7 m w.e. (MT07);
- 1077 for the telescope at the level of 20 m w.e. (MT20);
- 1077 for the telescope at the level of 40 m w.e (MT40).

Then we found averages for the entire time interval of interest for each channel of the complex, relative to which we estimated intensity variations (in %). Variables (pressure, surface, mass average temperatures, and temperatures at 16 isobars) were presented as deviations (changes) relative to the averages of these variables for the same period (from January 2016 to December 2018). Figure 1 shows raw data for four levels of muon detection.

Table 1 lists some parameters of the raw data.

DATA ANALYSIS AND RESULTS

Multivariate regression

The muon intensity variation observed consists of variations caused by variations in atmospheric pressure, surface layer temperature, integral air temperature effect, and primary cosmic rays. Represent the equation for muon intensity variations as a linear multivariate regression equation

$$\delta J_{\mu}(t) = \beta \Delta h(t) + \alpha_{surf} \Delta T_{surf}(t)\left[h(t) - 950\right] + \\ + \alpha_{ma} \Delta T_{ma}(t) + \gamma \delta J_{n}(t), \quad (1)$$

where $\delta J_{\mu}(t) = \dfrac{J_{\mu}(t) - \overline{J}_{\mu}}{\overline{J}_{\mu}} \cdot 100$ is the muon intensity variation (in %) (resultant factor y); $\Delta h = h(t) - h_0$ are variations in atmospheric pressure (factor x_1); $\Delta T_{surf}(t) = T_{surf}(t) - \overline{T}_{surf}$ are variations in variable mass layer temperature (factor x_2); $\Delta T_{ma}(t) = T_{ma}(t) - \overline{T}_{ma}$ are variations in mass average air temperature (factor x_3); $\delta J_{n}(t) = \dfrac{J_{n}(t) - \overline{J}_{n}}{\overline{J}_{n}}$ are neutron component intensity variations (data from the neutron monitor in Yakutsk), corrected for atmospheric pressure variations (factor x_4). There are also regression coefficients in Expression (1): α_{surf} is the temperature coefficient for the surface temperature; α_{ma} is the temperature coefficient for the mass average air temperature; β is the barometric coefficient; γ is the regression coefficient with neutron monitor data corrected for atmospheric pressure variations and reflecting primary CR variations. The multivariate regression (MVR) coefficients in (1) were found as in [Yanchukovsky, Kuzmenko, 2018], using the method of representing the regression equation on a standardized scale [Gorlach, 2006] and the least square method [Korn, Korn, 1984]. The regression coefficients thus found are presented in Table 2.

The regression coefficients γ were refined during large Forbush decreases in CRs, which occurred during the period of interest (in July and September 2017). The temperature coefficients for the variable mass layer α_{surf} were refined using the method of pair correlation between $\Delta T_{surf}(t)$ and the left-hand side of the expression

$$\frac{\delta J_{surf}(t)}{h(t) - 950} = \\ = \frac{\delta J_{\mu}(t) - \beta \Delta h(t) - \gamma \delta J_{n}(t) - \alpha_{ma} \Delta T_{ma}(t)}{h(t) - 950} = \\ = \alpha_{ma} \Delta T_{ma}(t) \quad (2)$$

For the continuous dataset from the beginning of 2016 to the end of 2018, α_{surf} was $-3.18 \cdot 10^{-4}$ for the vertical with a correlation coefficient of –0.2907, for $\dfrac{\delta J_{surf}(t)}{h(t) - 950}$ $\sigma = 0.0219$, and for $\Delta T_{surf}(t)$ $\sigma = 20.0053$.

The coefficients β, α_{surf}, α_{ma}, γ we have found allow us to identify the integral temperature effect (temperature component) in the muon intensity variations $\delta J_{\mu}(t)$:

$$\alpha_{ma} \Delta T_{ma}(t) = \delta J_{\mu}(t) - \beta \Delta h(t) - \\ - \alpha_{surf} \Delta T_{surf}(t) - \gamma \delta J_{n}(t). \quad (3)$$

The integral temperature effect is caused by variations in the atmospheric temperature at 16 isobars:

$$\alpha_{ma} \Delta T_{ma}(t) = \sum_{i=1}^{16} \alpha_i \Delta T_i(t). \quad (4)$$

Here $\Delta T_i(t) = T_i(t) - \overline{T}_i$ are atmospheric temperature variations at the i-th isobar; α_i is the regression coefficient or temperature coefficient for the i-th isobar.

The temperature coefficients α_i in MVR were obtained by presenting multivariate regression equations on a standardized scale, followed by solving a system of linear equations and using the least square method [Yanchukovsky, Kuzmenko, 2018]. The temperature coefficients obtained using MVR for five directions of the muon telescope MT00 are listed in Table 3.

For the least square method, the accuracy in estimating temperature coefficients was $2.5 \cdot 10^{-5}$. For the muon intensity temperature coefficient density, the weight coefficient determined by the relative mass of each atmospheric layer is taken into account: $\Delta h_i \Big/ \sum_{i=1}^{16} \Delta h_i$.

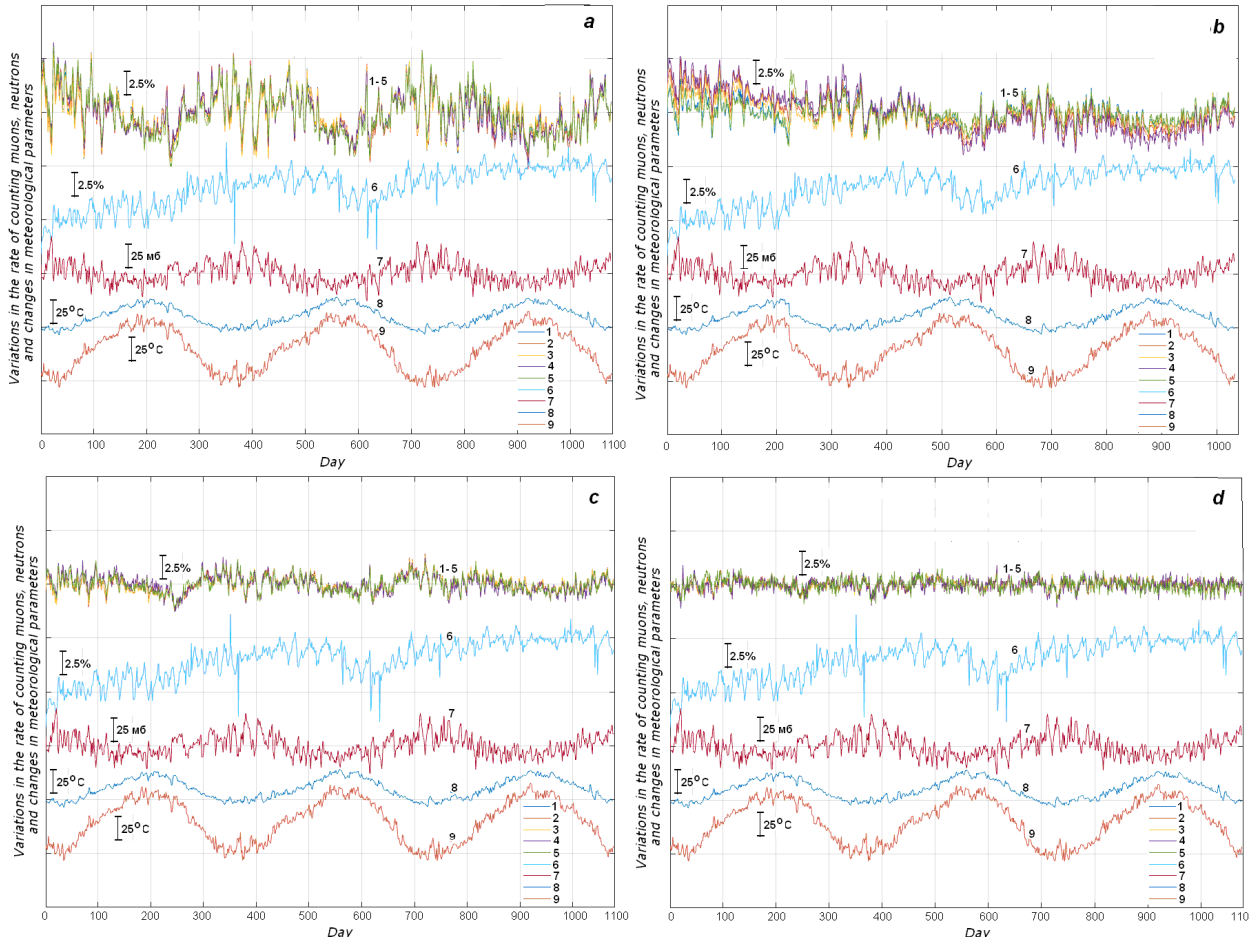

Figure 1. Variations in the counting rate of muons on Earth's surface (*a*) and under the ground at depths of 7 (*b*), 20 (*c*), and 40 m w.e. (*d*) from the vertical (curve 1), N30 (curve 2), S30 (curve 3), N60 (curve 4), S60 (curve 5), and of NM neutrons (curve 6), as well as variations in atmospheric pressure (curve 7), mass average air temperature (curve 8), and surface layer temperature (curve 9) for the period from January 2016 to December 2018

Table 1

Characteristics of raw data

Detection channels			0	N30	S30	N60	S60
Daily average count rate	h^{-1}	MT00	4300.97	2494.61	2489.94	1563.26	1524.43
		MT07	4171.44	2391.73	2443.97	1725.92	1550.17
		MT20	4053.07	1207.58	1245.89	816.11	910.11
		MT40	3587.53	2251.81	2107.88	399.11	367.85
	min^{-1}	NM	1701.97				
Conversion factor		MT00	256	128	128	16	16
		MT07	128	64	64	8	8
		MT20	64	64	64	8	8
		MT40	32	16	16	8	8
		NM	8				
Statistical error, %		MT00	0.019	0.036	0.036	0.129	0.130
		MT07	0.028	0.052	0.052	0.174	0.183
		MT20	0.04	0.073	0.072	0.252	0.239
		MT40	0.06	0.107	0.111	0.361	0.376
		NM	0.022				

The average meteorological parameters for the entire period were:

- 1002.33 mb for the atmospheric pressure;
- –30.86 °C for the mass average temperature;
- –5.67 °C for the variable mass layer temperature (surface layer).

Table 2

Regression coefficients for MT00, MT07, MT20, and MT40 channels

Coefficient	MT	0	N30	S30	N60	S60
β, %/mb	00	–0.189 ±0.0027	–0.187 ±0.003	–0.191 ±0.0034	–0.164 ±0.004	–0.175 ±0.006
	07	–0.109 ±0.0033	–0.117 ±0.004	–0.109 ±0.0038	–0.117 ±0.0045	–0.093 ±0.0032
	20	–0.076 ±0.0018	–0.074 ±0.002	–0.078 ±0.0023	–0.069 ±0.0024	–0.075 ±0.003
	40	–0.053 ±0.001	–0.052 ±0.001	–0.052 ±0.001	–0.046 ±0.0013	–0.048 ±0.0014
α_{ma}, %/°C	00	–0.225 ±0.0018	–0.230 ±0.002	–0.219 ±0.0019	–0.245 ±0.004	–0.251 ±0.0045
	07	–0.125 ±0.0023	–0.134 ±0.003	–0.120 ±0.0031	–0.157 ±0.0047	–0.107 ±0.0029
	20	–0.086 ±0.0022	–0.084 ±0.002	–0.087 ±0.0022	–0.084 ±0.0022	–0.088 ±0.0022
	40	–0.029 ±0.0007	–0.029 ±0.001	–0.029 ±0.0008	–0.027 ±0.0013	–0.035 ±0.0014
γ	00	0.368 ±0.008	0.370 ±0.009	0.353 ±0.009	0.330 ±0.016	0.300 ±0.017
	07	0.289 ±0.0082	0.289 ±0.009	0.261 ±0.0096	0.201 ±0.028	0.156 ±0.034
	20	0.192 ±0.0089	0.218 ±0.017	0.174 ±0.017	0.137 ±0.057	0.175 ±0.067
	40	0.123 ±0.0092	0.113 ±0.018	0.112 ±0.018	0.080 ±0.062	0.089 ±0.062
$\alpha_{surf}10^{-4}$, %/°C		–3.18 ±0.32	–3.57 ±0.41	–3.41 ±0.43	–3.61 ±0.68	–3.70 ±0.7

Table 3

Temperature coefficients and their densities of the muon telescope MT00 (MVR method)

i	h_i, mb	00 α_i 10^{-4}	N30 α_i 10^{-4}	S30 α_i 10^{-4}	N60 α_i 10^{-4}	S60 α_i 10^{-4}	Δh_i, mb	00 w_i 10^{-3}	N30 w_i 10^{-3}	S30 w_i 10^{-3}	N60 w_i 10^{-3}	S60 w_i 10^{-3}
1	925	–197	–203	–201	–233	–264	50	–375	–387	–382	–444	–502
2	850	–319	–326	–322	–374	–424	100	–303	–310	–306	–356	–403
3	700	–331	–344	–339	–393	–445	150	–211	–218	–215	–249	–282
4	600	–218	–225	–221	–258	–291	100	–207	–214	–211	–245	–277
5	500	–240	–247	–244	–283	–320	100	–228	–235	–232	–269	–304
6	400	–231	–238	–239	–272	–308	100	–220	–226	–227	–259	–293
7	300	–172	–176	–174	–202	–229	75	–218	–223	–220	–256	–290
8	250	–116	–119	–118	–137	–155	50	–221	–227	–224	–261	–295
9	200	–113	–119	–118	–137	–155	50	–221	–226	–224	–260	–294
10	150	–112	–116	–114	–133	–150	50	–214	–220	–217	–253	–285
11	100	–105	–108	–108	–125	–142	45	–223	–229	–228	–265	–299
12	70	–47	–48	–48	–56	–62	20	–222	–228	–227	–264	–296
13	50	–48	–50	–49	–57	–64	20	–231	–237	–235	–272	–307
14	30	–34	–36	–35	–41	–46	15	–218	–225	–224	–260	–291
15	20	–20	–19	–19	–22	–25	10	–188	–185	–183	–213	–239
16	10	–17	–18	–21	–24	–27	15	–110	–118	–135	–157	–176

Figure 2 illustrates the temperature coefficient densi ty distributions found by the MVR method for muons detected by the telescope MT00 on Earth's surface.

Regression on principal components

When studying the temperature effect of muons detected by Yakutsk complex of underground detectors, we employed the multivariate regression (MVR) and the principal component method [Aivazyan et al., 1989]. When considering regression on principal components (RPC) [Jolliffe, 2002; Gorban et al., 2007], we applied projection methods on latent structures (PLS) [Esbensen, 2005; Pomerantsev, 2014]. This is due to the fact that variables (temperatures at 16 isobars) should be considered as correlated factors. To develop a system of linear equations

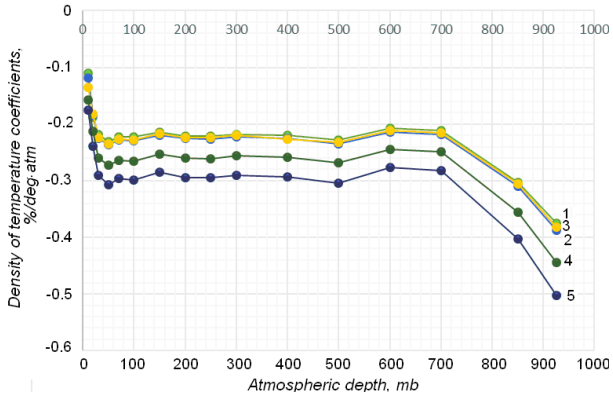

Figure 2. Distribution of temperature coefficient density for muons detected by the telescope MT00 from the vertical (curve 1), at an angle of 30° to the vertical from directions N (curve 2) and S (curve 3), as well as at an angle of 60° from directions N (curve 4) and S (curve 5)

in the space of principal components (PC), we used the PLS method.

Both RPC and PLS methods involve creating a space N of implicit parameters having zero correlation coefficients between themselves so that the percentage of information content of raw data is distributed among each of them from larger to smaller, providing in total 100 % of the information of the original sample.

By analyzing calculated values for measures of informativeness of contributions of each component, we estimate the number of PC whose raw data variations contain basic information. According to this estimate, matrices of transfer to a reduced space are constructed. To create this space, an orthogonal transformation into a new coordinate system is necessary for which the following conditions would be true:

- the sample variance of data along the first coordinate is maximum (this coordinate is also known as the first principal component);
- the sample variance of data along the second coordinate is maximum under the condition of orthogonality to the first coordinate (the second principal component);
- the sample variance of data along the k-th coordinate is maximum under the condition of orthogonality to the first k–1 coordinates.

Most of the variations in the original sample generally occur along the first coordinate. The variations related to the next parameter are observed along the second coordinate, etc. Such a space of implicit parameters is created provided that the relationship between responses and input data is maximum. On this basis, we can easily generate a modified representation of original regression, and then, taking into account the calculated informativeness for each new coordinate, determine the optimal data dimension that meets the specified accuracy criteria.

By solving a series of regressions on reduced dimension modified data, we find coefficients of the relationship between responses and input data. Having a set of responses and applying the same transformation, used for the training sample, to them, we can get a set of modified responses. The regression coefficients and modified responses are used to restore the reduced dimension modified input data.

Applying the inverse transform to the data, we calculate initial input data.

The use of the MPC, PLS-1, and PLS-2 methods for solving such problems has been discussed in [Kuzmenko, Yanchukovsky, 2015]. When comparing the results obtained by different methods, we concluded that the PLS-2 method yields the best result. The Unscrambler X software [https://www.aspentech.com/ru/products/apm/aspen-unscrambler] allows us to use the PLS-2 method to calculate by four algorithms. It has also been shown [Yanchukovsky, Kuzmenko, 2018] that for such problems the KERNEL PLS algorithm [Lindgren et al., 1993; de Jong, Ter Braak, 1994; Dayal, McGregor, 1997] is optimal because it is better suited for a large number of samples than other algorithms — in our case, thousands of samples with several variables (the number of samples here means the number of values in data series for each variable).

Figure 3 presents the results of calculation of variances for the selected PC vectors, PC vector eigenvalues, and measures of informativeness of transformed data with increasing number of principal components.

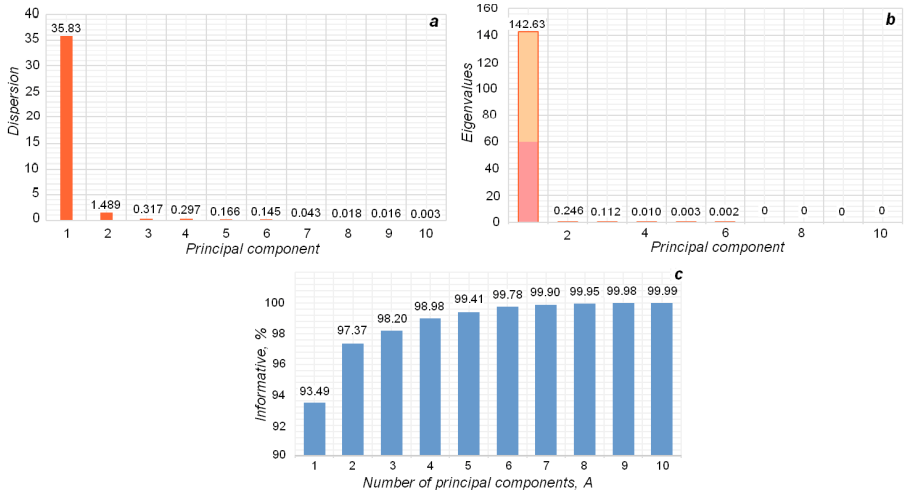

Figure 3. Informativeness of transformed data with increasing number of principal components: variance of PC vectors (*a*); PC eigenvalues (*b*); measure of informativeness of transformed data with increasing number of principal components (*c*)

It is shown that the problem of multicollinearity and input data matrix dimension reduction can be solved through transition to the space of principal components. Using the calculated measures of informativeness of contributions of each component, we estimate the number of principal components whose initial data variations contain basic information (in this case, the optimal PC number is two). This estimate is used to construct matrices of transition to a reduced space. To clarify the choice of the PC number, we employ the selected temperature component of $\alpha_{ma}\Delta T_{ma}$ for a ground muon telescope from the vertical.

Figure 4 illustrates temperature coefficient density distributions for muons in the atmosphere, found by the PLS-2 method for a different number of principal components.

For the maximum number of principal components equal to the total number of variables (temperature at 16 isobars), the result (curve 5) completely coincides with those (curve 6) obtained by the MVR method. One principal component contains 93 % of the information that increases by only 4 % for two PC, and by 0.8 % for three PC (see Figure 3). With a further increase in the number of principal components, the informativeness increases slightly, whereas the noise contribution probability increases markedly. With a large number of principal components, the PLS-2 method loses its advantages over the MVR method: the results obtained are almost identical (see Figure 4). This confirms that two principal components should be used in this problem. The temperature coefficients and their densities derived by the PLS-2 method for ground (MT00) and underground muon telescopes at depths of 7 (MT07), 20 (MT20), and 40 m w.e (MT40) are listed in Tables 4, 5, 6, and 7 respectively.

Distributions of temperature coefficient density for muons in the atmosphere detected by telescopes on Earth's surface and under the ground are illustrated in Figure 5.

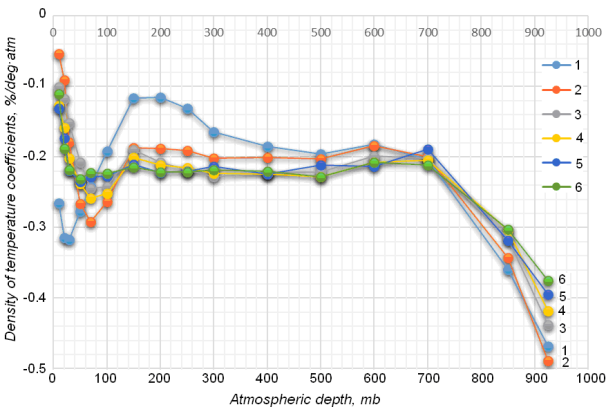

Figure 4. Distributions of temperature coefficient density for the telescope MT00 Vertical, found using a different number of principal components: one PC — curve 1; two PC — curve 2; three PC — curve 3; five PC — curve 4; 16 PC — curve 5; curve 6 is the result obtained by the MVR method

Table 4

Temperature coefficients and their densities of the muon telescope MT00

i	h_i, mb	00 $\alpha_i\,10^{-4}$	N30 $\alpha_i\,10^{-4}$	S30 $\alpha_i\,10^{-4}$	N60 $\alpha_i\,10^{-4}$	S60 $\alpha_i\,10^{-4}$	Δh_i, mb	00 $w_i\,10^{-3}$	N30 $w_i\,10^{-3}$	S30 $w_i\,10^{-3}$	N60 $w_i\,10^{-3}$	S60 $w_i\,10^{-3}$
1	10	–8	–8	–8	–9	–9	15	–54	–53	–51	–58	–59
2	20	–10	–10	–9	–11	–11	10	–91	–94	–89	–101	–103
3	30	–28	–29	–28	–31	–32	15	–179	–184	–175	–197	–202
4	50	–56	–57	–54	–62	–63	20	–266	–273	–259	–292	–299
5	70	–61	–63	–60	–68	–69	20	–292	–300	–284	–321	–329
6	100	–125	–128	–121	–137	–140	45	–263	–270	–256	–290	–296
7	150	–99	–101	–96	–109	–116	50	–187	–192	–183	–206	–220
8	200	–99	–102	–97	–109	–112	50	–188	–193	–184	–207	–212
9	250	–101	–103	–98	–111	–113	50	–191	–196	–186	–210	–215
10	300	–160	–162	–153	–173	–178	75	–202	–204	–193	–218	–224
11	400	–211	–213	–202	–229	–234	100	–201	–203	–192	–217	–223
12	500	–214	–217	–206	–232	–239	100	–203	–206	–195	–221	–227
13	600	–194	–199	–188	–213	–219	100	–184	–189	–179	–202	–208
14	700	–317	–326	–309	–349	–359	150	–200	–205	–195	–220	–226
15	850	–361	–370	–351	–397	–406	100	–343	–352	–334	–377	–386
16	925	–257	–306	–251	–283	–290	50	–489	–502	–476	–538	–551

Table 5

Temperature coefficients and their densities of the muon telescope MT07

i	h_i, mb	00 α_i 10^{-4}	N30 α_i 10^{-4}	S30 α_i 10^{-4}	N60 α_i 10^{-4}	S60 α_i 10^{-4}	Δh_i, mb	00 w_i 10^{-3}	N30 w_i 10^{-3}	S30 w_i 10^{-3}	N60 w_i 10^{-3}	S60 w_i 10^{-3}
1	10	–4	–4	–3	–4	–3	15	–23	–24	–22	–28	–21
2	20	–5	–5	–4	–6	–4	10	–42	–45	–40	–53	–39
3	30	–14	–15	–14	–18	–13	15	–90	–97	–87	–114	–80
4	50	–29	–32	–28	–37	–26	20	–140	–152	–135	–178	–123
5	70	–33	–36	–32	–42	–28	20	–158	–171	–152	–200	–135
6	100	–68	–73	–65	–86	–58	45	–143	–155	–138	–182	–123
7	150	–53	–58	–52	–68	–46	50	–102	–110	–98	–129	–87
8	200	–54	–58	–52	–68	–46	50	–102	–110	–98	–129	–87
9	250	–54	–59	–53	–69	–47	50	–103	–112	–100	–131	–89
10	300	–86	–93	–83	–109	–74	75	–109	–118	–105	–138	–93
11	400	–115	–124	–111	–146	–98	100	–109	–118	–105	–138	–93
12	500	–117	–126	–113	–148	–100	100	–111	–120	–107	–141	–95
13	600	–107	–116	–104	–136	–92	100	–102	–110	–98	–129	–87
14	700	–175	–190	–169	–222	–150	150	–111	–120	–107	–141	–95
15	850	–200	–216	–193	–254	–171	100	–190	–205	–183	–241	–163
16	925	–133	–154	–137	–181	–122	50	–271	–293	–261	–343	–232

Table 6

Temperature coefficients and their densities of the muon telescope MT20

i	h_i, mb	00 α_i 10^{-5}	N30 α_i 10^{-5}	S30 α_i 10^{-5}	N60 α_i 10^{-5}	S60 α_i 10^{-5}	Δh_i, mb	00 w_i 10^{-3}	N30 w_i 10^{-3}	S30 w_i 10^{-3}	N60 w_i 10^{-3}	S60 w_i 10^{-3}
1	10	–31	–31	–31	–30	–32	15	–20	–19	–20	–19	–20
2	20	–36	–36	–36	–35	–37	10	–34	–34	–35	–33	–35
3	30	–107	–105	–108	–104	–110	15	–68	–66	–68	–66	–70
4	50	–211	–207	–213	–205	–218	20	–100	–98	–101	–97	–103
5	70	–232	–228	–234	–225	–239	20	–110	–108	–111	–107	–114
6	100	–471	–462	–474	–457	–485	45	–99	–97	–100	–96	–102
7	150	–373	–365	–375	–362	–384	50	–71	–69	–71	–69	–73
8	200	–374	–367	–377	–364	–386	50	–71	–70	–72	–69	–73
9	250	–379	–372	–382	–368	–391	50	–72	–71	–73	–70	–74
10	300	–593	–581	–597	–575	–610	75	–75	–74	–76	–73	–77
11	400	–786	–770	–792	–763	–810	100	–75	–73	–75	–72	–77
12	500	–797	–782	–803	–775	–821	100	–76	–74	–76	–74	–78
13	600	–733	–718	–744	–710	–754	100	–70	–68	–71	–67	–72
14	700	–1194	–1170	–1203	–1159	–1268	150	–76	–74	–76	–73	–80
15	850	–1363	–1336	–1366	–1324	–1374	100	–129	–127	–130	–126	–130
16	925	–882	–864	–888	–856	–892	50	–167	–164	–169	–163	–169

Table 7

Temperature coefficients and their densities of the muon telescope MT40

i	h_i, mb	00 α_i 10^{-5}	N30 α_i 10^{-5}	S30 α_i 10^{-5}	N60 α_i 10^{-5}	S60 α_i 10^{-5}	Δh_i, mb	00 w_i 10^{-4}	N30 w_i 10^{-4}	S30 w_i 10^{-4}	N60 w_i 10^{-4}	S60 w_i 10^{-4}
1	10	–11	–10	–10	–10	–13	15	–68	–66	–67	–62	–80
2	20	–12	–12	–12	–11	–15	10	–119	–115	–118	–109	–140
3	30	–37	–35	–37	–34	–44	15	–232	–225	–232	–215	–276
4	50	–72	–70	–72	–67	–86	20	–344	–333	–344	–319	–409
5	70	–78	–77	–80	–74	–95	20	–370	–366	–378	–350	–450
6	100	–161	–156	–161	–149	–192	45	–341	–330	–341	–315	–405
7	150	–128	–124	–128	–118	–152	50	–243	–235	–243	–225	–289
8	200	–128	–124	–128	–118	–153	50	–244	–236	–244	–226	–290
9	250	–130	–126	–130	–120	–155	50	–247	–239	–247	–229	–294
10	300	–203	–197	–203	–188	–242	75	–257	–249	–257	–238	–306
11	400	–269	–261	–269	–249	–320	100	–256	–248	–256	–237	–304
12	500	–276	–261	–275	–254	–325	100	–262	–248	–261	–241	–309
13	600	–253	–268	–253	–233	–298	100	–240	–255	–240	–221	–283
14	700	–412	–361	–412	–379	–486	150	–261	–229	–261	–240	–308
15	850	–466	–453	–467	–433	–556	100	–443	–430	–444	–411	–528
16	925	–333	–323	–333	–308	–449	50	–632	–613	–633	–586	–853

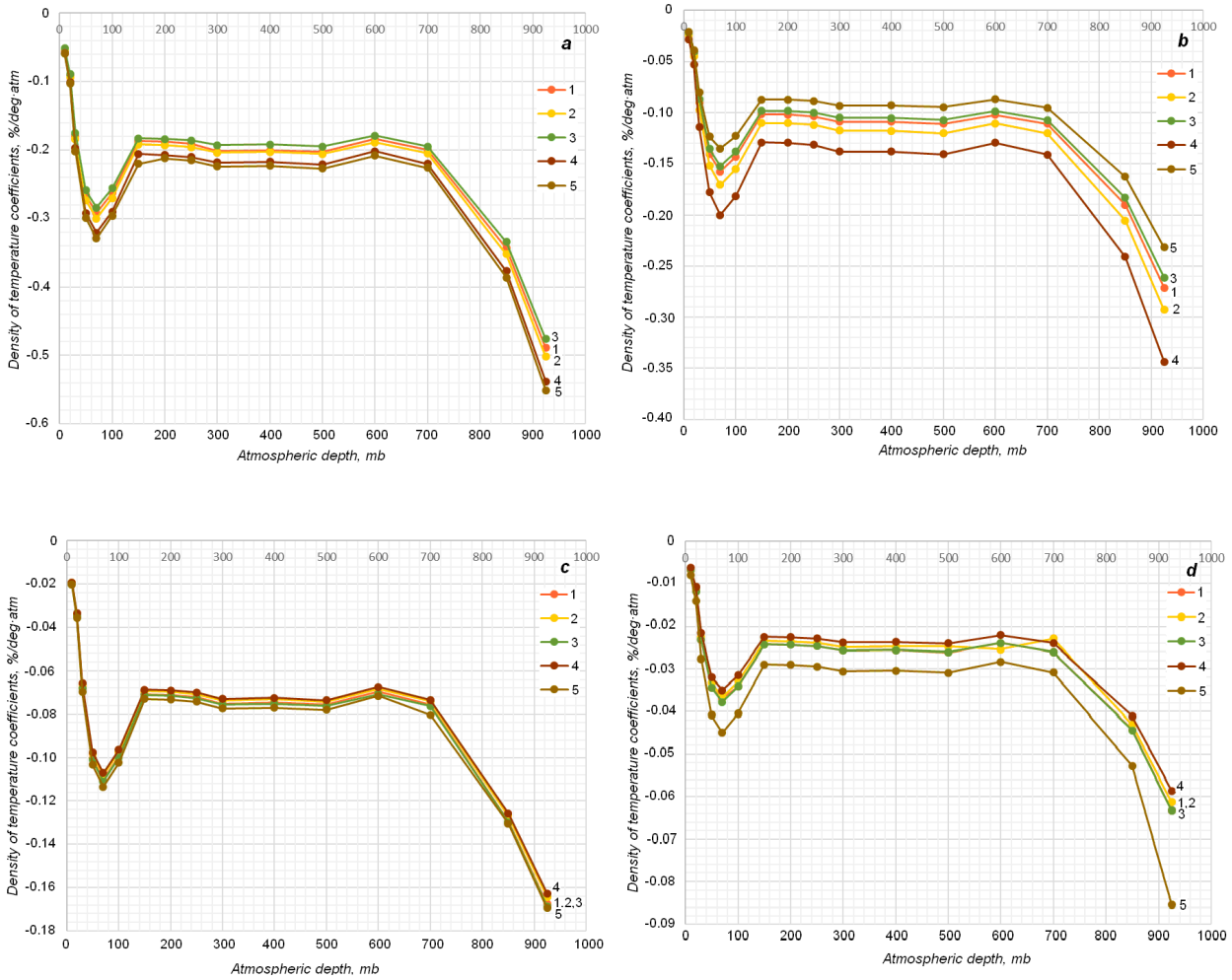

Figure 5. Distributions of temperature coefficient density for muons detected on Earth's surface (*a*) and under the ground at depths of 7 (*b*), 20 (*c*), and 40 m w.e. (*d*) from the vertical (curve 1), N30 (curve 2), S30 (curve 3), N60 (curve 4), S60 (curve 5)

DISCUSSION

The integral temperature effect of muons in the atmosphere, found taking into account the temperature coefficient density distribution and from the coefficient for the mass average temperature, should be the same within the limits provided by the accuracy of estimated coefficients. Given this, the average temperature coefficient density from 0 to 950 mb should correspond to the coefficient for the mass average temperature. The test results for the MVR and PLS-2 methods are presented in Table 8.

Figure 6 shows for comparison the density distributions of the temperature coefficients derived by the MVR and PLS-2 methods for the vertical of the telescopes MT00 in Yakutsk and Novosibirsk [Yanchukovsky, Kuzmenko, 2018].

When estimating α_i and w_i for Novosibirsk muon telescope, we used aerological sounding data from the weather station Bugrinskaya Roshcha (Novosibirsk). The sounding data have many gaps, especially in winter for high altitudes, and are presented only for 11 isobars with a rate of sounding twice a day. The geomagnetic cutoff threshold for the cosmic ray station (CRS) Novosibirsk is 2.91 GeV; and for CRS Yakutsk, 1.65 GeV. The telescope MT00 in Yakutsk differs in design from the muon telescope in Novosibirsk, has no screen, and has a wider directional pattern. Nevertheless, we observe agreement between the results obtained.

We [Kuzmenko, Yanchukovsky, 2017] have calculated the expected temperature coefficient densities for the complex of underground muon telescopes in Yakutsk. Let us compare the results obtained with the results of calculations in Figure 7, where we show the values found as averages for N30, S30 and N60, S60 for 30° and 60° zenith angles. Figure 7 demonstrates that the results obtained agree well with the calculated ones.

The resulting distributions of temperature coefficient density for different zenith angles of detection at each of the observation levels differ slightly (curves 1, 2, 3 in Figure 6). It is easy to observe in the initial data (Figure 1)

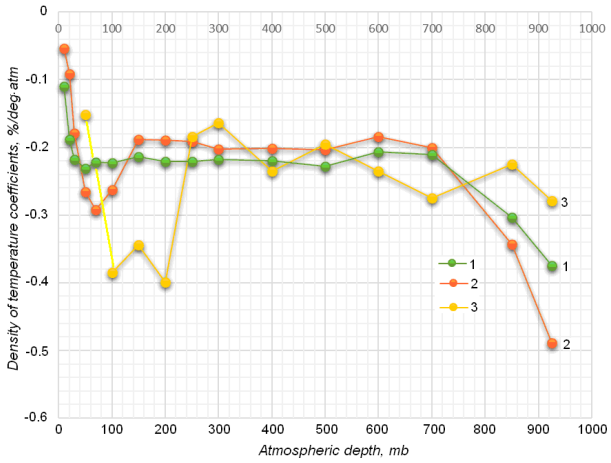

Figure 6. Distribution of temperature coefficient density in the atmosphere for vertical of the muon telescope MT00 in Yakutsk (MVR method (curve 1); PLS-2 method (curve 2)) and the muon telescope in Novosibirsk (curve 3)

that the amplitudes of variations in the muon count rate from different directions differ little, and for the level of 20 m w.e. there are almost no differences. The main reason for this is design parameters of the telescopes [Project..., 2004; Grigoryev et al., 2011; Starodubtsev et al., 2013, 2016], in which the apertures for the vertical and the directions at an angle to the vertical overlap, and for the 30°zenith angle overlap completely. At the same time, apertures of the telescopes also depend on the azimuth angle. Another reason is the principle of developing an event selection system [Project..., 2004], where counters are combined in pairs into trays (switched into one discriminator amplifier). Further, in the event selection system (in coincidence circuits), the signals from each of these counters are examined independently, and the resolving time in these coincidence circuits is unreasonably long [Project ..., 2004], which leads to a great contribution of random coincidences.

Table 8

Test results for the MVR and PLS-2 methods

		00		N30		S30		N60		S60	
		MVR	PLS	MVR	PLS	MVR	PLS	MVR	PLS	MVR	PLS
MT00	$\overline{w_i}$	–0.226	–0.221	–0.232	–0.226	–0.231	–0.215	–0.268	–0.242	–0.302	–0.249
	α_{ma}	–0.225±0.0018		–0.230±0.002		–0.21±0.0019		–0.245±0.004		–0.251±0.0045	
MT07	$\overline{w_i}$	–0.132	–0.119	–0.153	–0.129	–0.122	–0.115	–0.161	–0.151	–0.108	–0.103
	α_{ma}	–0.125±0.0023		–0.134±0.003		–0.120±0.0031		–0.157±0.0047		–0.107±0.0029	
MT20	$\overline{w_i}$	–0.085	–0.082	–0.083	–0.081	–0.086	–0.083	–0.083	–0.080	–0.088	–0.085
	α_{ma}	–0.086±0.0022		–0.084±0.002		–0.087±0.0022		–0.084±0.0022		–0.088±0.0022	
MT40	$\overline{w_i}$	–0.029	–0.029	–0.028	–0.028	–0.029	–0.029	–0.027	–0.027	–0.035	–0.035
	α_{ma}	–0.029±0.0007		–0.029±0.001		–0.029±0.0008		–0.027±0.0013		–0.035±0.0014	

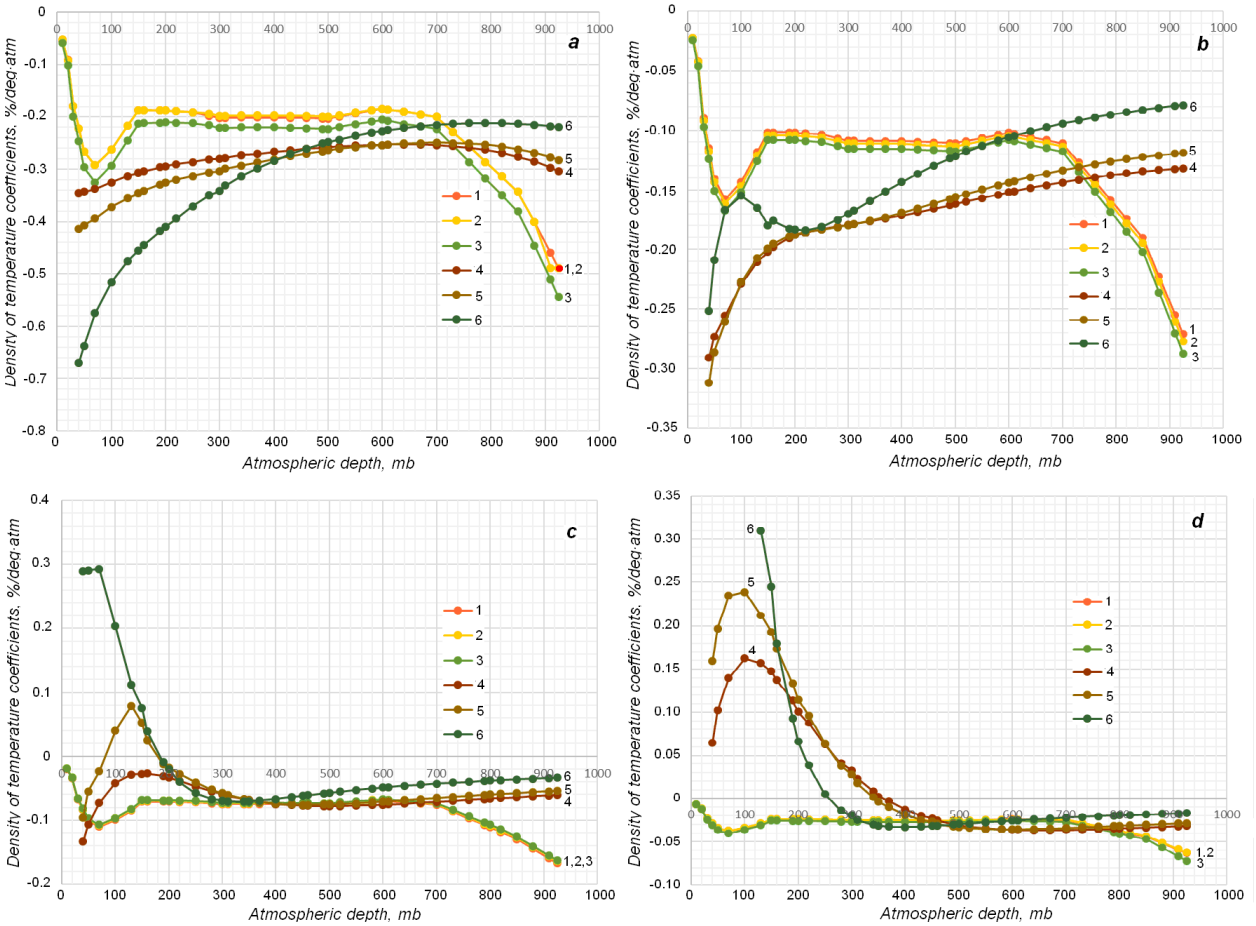

Figure 7. Distributions of temperature coefficient density for muons detected at zenith angles of 0 (curve 1), 30 (curve 2), and 60 (curve 3) obtained from continuous observations as well as from calculations for angles of 0 (curve 4), 30 (curve 5), and 60 (curve 6) on Earth's surface (*a*) and under the ground at depths of 7 (*b*), 20 (*c*), and 40 m w.e. (*d*) respectively

Figure 8 shows distributions of temperature coefficient density for muons detected from the vertical at various underground levels. The dependence of the temperature coefficient density on the muon detection depth under the ground is clear cut.

When muons are detected from the vertical, the negative temperature effect of muons decreases several times with increasing underground depth.

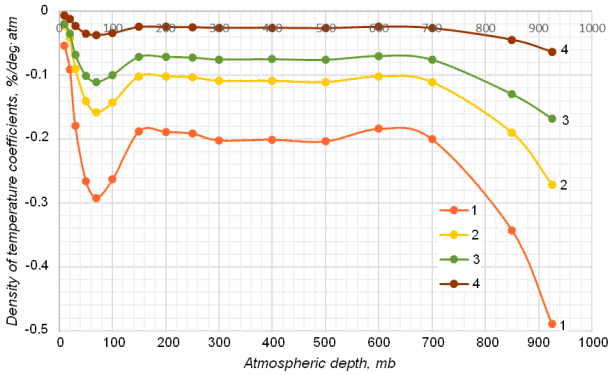

Figure 8. Distributions of temperature coefficient density for muons detected from the vertical on Earth's surface (curve 1) and under the ground at depths of 7 (curve 2), 20 (curve 3), and 40 m w.e. (curve 4)

CONCLUSION

From continuous observations of muons and atmospheric temperature measurements at different altitudes, we have found distributions of temperature coefficient density for muons detected on Earth's surface and under the ground. It is usually difficult to experimentally estimate distributions of temperature coefficient density because temperature variations in different atmospheric layers are correlated. We have therefore employed different factor analysis methods. We have made a comparative estimate of the results of different analysis methods. The experimental results were compared with the calculation ones.

The temperature coefficient density distributions obtained for muons in the atmosphere allow us to take into account the existing temperature effect of muons detected under the ground. There is a pronounced dependence of the temperature effect of muons on the depth of their detection under the ground, which makes it possible to use cosmic rays to diagnose the pressure-temperature conditions of the atmosphere.

The work was financially supported by the Ministry of Science and Higher Education of the Russian Federation (Project FWZZ-2022-0019). The results were obtained using the equipment of URF-85 "Russian National Network of Cosmic Ray Stations" [http://www.ckp-rf.ru/usu/433536/].

REFERENCES

Aivazyan S.A., Bukhshtaber V.M., Enyukov I.S., Meshalkin L.D. *Prikladnaya Statistika. Klassifikatsiya i snizhenie razmernosti* [Applied statistics. Classification and dimension lowering]. Moscow, Finansy i statistika Publ., 1989, 607 p. (In Russian).

Berkova M., Belov A., Eroshenko E., Yanke V. Temperature effect of the muon component of cosmic ray and practical possibilities of its accounting. *Proc. 21st ECRC*. 2008, pp. 123–126.

Dayal B.S., McGregor J.F. Improved PLS Algorithms. *J. Chemometrics*. 1997, vol. 11, pp. 73–85. DOI: 10.1002/(SICI)1099-128X(199701)11:1<73::AID-CEM435>3.0.CO;2-%23.

de Jong S., Ter Braak C. Comments on the PLS kernel algorithm. *J. Chemometrics*. 1994, vol. 8, pp. 169–174.

Dmitrieva A.N., Kokoulin R.P., Petruhin A.A., Timashov D.A. Temperature coefficients for muons under different zenith angles. *Izv. RAN. Ser. Fiz* [Bulletin of the Russian Academy of Sciences. Physics], 2009, vol. 73, no. 3, pp. 371–374. (In Russian).

Dorman L.I. *Variatsii kosmicheskikh luchei* [Variations of Cosmic Rays]. Moscow, Gostechizdat Publ., 1957, 285 p. (In Russian).

Dorman L.I. *Meteorologicheskie effekty kosmicheskikh luchei* [Meteorological Effects of Cosmic Rays]. Moscow, Nauka Publ., 1972, 211 p. (In Russian).

Dorman L.I., Yanke V.G. On theory of meteorological effects of cosmic rays. *Izvestiya AN SSSR. Ser. Fizicheskaya* [Bulletin of the Academy of Sciences of USSR. Physics], 1971, vol. 35, no. 12, pp. 2556–2570. (In Russian).

Esbensen K. *Analis mnogomernykh dannykh. Izbrannye glavy* [Analysis of Multidimensional Data. Selected Chapters]. Chernogolovka, IPHF RAN Publ., 2005, p. 160. (In Russian).

Gerasimova S.K., Gololobov P.Y., Grigor'ev V.G., Zverev A.S., Starodubtsev S.A., Egorov A.G., Neustroev N.I., Mikheev A.A., Sorokin E.E., Karmadonov A.Y., Pakhmullov A.V. Muon telescope based on scintillation counters. *Instruments and Experimental Technique*. 2021, vol. 64, no. 4, pp. 558–565. DOI: 10.1134/S0020441221040047.

Gorlach B.A. *Matematika* [Mathematics]. Moscow, Nauka Publ., 2006, 911 p. (In Russian).

Grigoryev V.G., Starodubtsev S.A., Krymsky G.F., Krivoshapkin P.A., Timofeev V.E., Prikhodko A.N., Karmadonov A.YA. Modern Yakutsk Cosmic Ray Spectrograph after A.I. Kuzmin. *Proc. 32nd International Cosmic Ray Conference, Beijing.* 2011, vol. 11, pp. 252–255. DOI: 10.7529/ICRC2011/V11/0360.

Lindgren F., Geladi P., Wold S. The kernel algorithm for PLS. *J. Chemometrics*. 1993, vol. 7, pp. 45–59. DOI: 10.1002/cem.1180070104.

Gorban A.N., Kegl B., Wunsch D., Zinovyev A.Y. *Principal Manifolds for Data Visualization and Dimension Reduction*. Springer, 2007, 340 p. (Lecture Notes in Computational Science and Engineering, vol. 58).

Jolliffe I.T. *Principal Component Analysis*. New York, Springer, 2002, 488 p. (Springer Series in Statistics).

Korn G., Korn T. *Spravochnik po matematike dlya nauchnykh rabotnikov i inzhenerov* [A Handbook of Mathematics for Scientists and Engineers]. Moscow, Nauka Publ., 1984, 831 p. (In Russian). (English edition: Korn G., Korn T. Mathematical Handbook for Scientists and Engineers. New York, McGraw-Hill Inc., 1968, 1130 p.)

Kuzmenko V.S., Yanchukovsky V.L. Determination of the density of temperature coefficients for muons in the atmosphere. *Solnechno-zemnaya fizika* [Solar-Terrestrial Physics]. 2015, vol. 1, no. 2, pp. 91–96. (In Russian). DOI: 10.12737/10403.

Kuzmenko V.S., Yanchukovsky V.L. Distribution of temperature coefficient density for muons in the atmosphere. *Solar-Terrestrial Physics*. 2017, vol. 3, iss. 4, pp. 104–116. DOI: 10.12737/19883.

Pomerantsev A.L. *Khemometrika v Excel: uchebnoe posobie.* [*Chemometrics in Excel: Tutorial*]. Tomsk, TPU Publ., 2014, 435 p. (In Russian).

Proekt modernizatsii Spektrograf cosmicheskikh luchei [Modernization project cosmic ray spectrograph]. Yakutsk, IKFIA RAN Publ., 2004, 37 p.

Starodubtsev S.A., Grigor'ev V.G., Isakov D.D., Karmadonov A.Ya., Pakhmulov A.V., Egorov A.G., Ksenofontov I.V. Modernization of the Yakutsk Cosmic Ray Spectrograph named after A.I. Kuzmin. *Trudy Vserossiyskoi konferentsii po solnechno-zemnoi fizike, posvyashchennoi 100-letiyu so dnya rozhdeniya chlena-korrespondenta RAN V.E. Stepanova* [Proceedings of the All-Russian Conference on Solar-Terrestrial Physics, dedicated to the 100th anniversary of the birth of Corresponding Member of the Russian Academy of Sciences V.E. Stepanova], Irkutsk, ISZF SO RAN Publ., 2013, pp. 289–293. (In Russian).

Starodubtsev S.A., Grigor'ev V.G., Gololobov P.Yu. Yakutsk Cosmic Ray Spectrograph named after V.I. A.I. Kuzmin: current state. *Sbornik trudov Vserossiyskoi konferentsii "Geliogeofizicheskie issledovaniya v Arktike"* [Proceedings of the All-Russian Conference "Heliogeophysical Research in the Arctic"] Murmansk, Polar Geophysical Institute Publ., 2016, pp. 125–129.

Yanchukovsky V.L., Kuzmenko V. Atmospheric effects of the cosmic-ray mu-meson component. *Solar-Terrestrial Physics*. 2018, vol. 4, iss. 3, pp. 76–82. DOI: 10.12737/szf-43201810.

URL: https://ikfia.ysn.ru/data/hecrlab/mt (accessed February 10, 2023).

URL: https://ikfia.ysn.ru/data/hecrlab/ipm (accessed February 10, 2023).

URL: http://crsa.izmiran.ru/phpmyadmin (accessed February 10, 2023; access for registered users).

URL: https://www.nco.ncep.noaa.gov/pmb/products/gfs (accessed February 10, 2023).

URL: https://www.aspentech.com/ru/products/apm/aspen-unscrambler (accessed February 10, 2023).

URL: http://www.ckp-rf.ru/usu/433536 (accessed February 10, 2023).

Original Russian version: Yanchukovsky V.L., published in Solnechno-zemnaya fizika. 2023. Vol. 9. Iss. 2. P. 60–70. DOI: 10.12737/szf-92202307.

How to cite this article

Yanchukovsky V.L. Temperature effect of muons registered under ground in Yakutsk by telescopes on gas-discharge counters. *Solar-Terrestrial Physics*. 2023. Vol. 9. Iss. 2. P. 55–65. DOI: 10.12737/stp-92202307.